

Entanglement Swapping with Storage and Retrieval of Light

Zhen-Sheng Yuan^{2,1}, Yu-Ao Chen^{1,2}, Bo Zhao¹, Shuai Chen¹, Jörg Schmiedmayer³ and Jian-Wei Pan^{1,2}

¹*Physikalisches Institut, Ruprecht-Karls-Universität Heidelberg, Philosophenweg 12, 69120 Heidelberg, Germany*

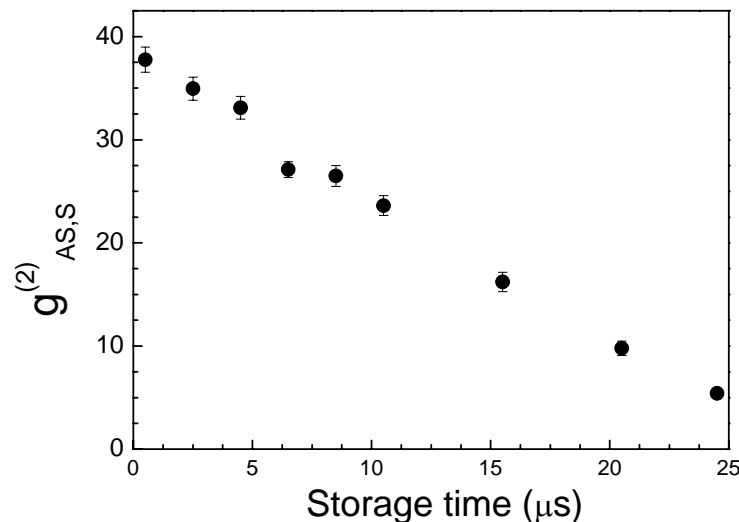
²*Hefei National Laboratory for Physical Sciences at Microscale and Department of Modern Physics, University of Science and Technology of China Hefei, Anhui 230026, China*

³*Atominstitut der österreichischen Universitäten, TU-Wien, A-1020 Vienna, Austria*

1. Atom-photon entanglement source

As discussed in the present paper, generating atom-photon entanglement is the first step to demonstrate a quantum repeater. We will provide here the information on the quality of the atomic-ensemble based quantum memory and of the atom-photon entanglement source.

Shown in Fig. 1 of the present paper, the collective excitations in either of the two spatial modes (labelled L for the left one and R for the right) are used as stationary qubits that are entangled with photonic qubits. That is, the entangling components are the polarization of the photon and the excitation of the spatial mode. We can investigate the two modes individually addressed by a specific polarization of the emitted single photons from either of the two spatial modes. For example, if vertical/horizontal (V/H) polarized light are chosen at the outputs of PBS1 and PBS2, the property of the L/R mode is being analyzed and can be operated separately.



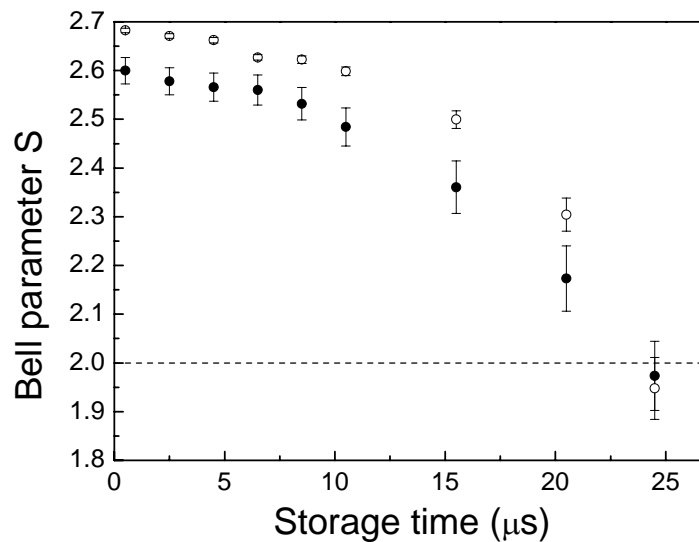
Supplementary Figure 1: The decay of cross correlation $g_{AS,S}^{(2)}$ with the storage time.

The detection probability of anti-Stokes photons is fixed at 2×10^{-3} .

The cross correlation function $g_{AS,S}^{(2)}$ can be used to characterize the property of a quantum memory. Theoretically, $g_{AS,S}^{(2)} = 1 + 1/\chi$, where χ is the excitation probability of an atomic ensemble. Neglecting the imperfections of the optics, the interference visibility V between anti-Stokes and Stokes photons can be obtained from an optimistic estimation as²⁸

$$V = \frac{g_{AS,S}^{(2)} - 1}{g_{AS,S}^{(2)} + 1}. \quad (\text{S1})$$

The cross correlation $g_{AS,S}^{(2)}$ decays along the storage time, which also causes decay of the visibility and therefore the atom-photon entanglement. Shown in Supplementary Figure 1, $g_{AS,S}^{(2)}$ for one spatial mode becomes lower than 6 when the storage time reaches 24 μs , indicating the visibility is lower than 71%.



Supplementary Figure 2: Decay of the S parameter in the Bell's inequality with the storage time at excitation rate of 2×10^{-3} . The solid dots are the measured data and the circles are calculated from the correlation function $g_{AS,S}^{(2)}$. The dashed line shows the classical bound $S=2$.

The atom-photon entanglement is written as Eqn. (1) and can be converted to the entanglement between the Stokes and anti-Stokes photons, Eqn. (2). It is verified by the measurement of the Bell's inequality,

$$S_{AS,S} = |E(\theta_{AS}, \theta_S) - E(\theta_{AS}, \theta'_S) - E(\theta'_{AS}, \theta_S) - E(\theta'_{AS}, \theta'_S)| \quad (\text{S2})$$

where $E(\theta_{AS}, \theta_S)$ is the correlation function, in which θ_{AS} and θ'_{AS} (θ_S and θ'_S) are the measured polarization bases of the anti-Stokes (Stokes) photon. During the measurement, the polarization settings are $(0^\circ, 22.5^\circ)$, $(0^\circ, -22.5^\circ)$, $(0^\circ, 22.5^\circ)$, and $(45^\circ, -22.5^\circ)$, respectively. The parameter S can be approximately estimated by $S = 2\sqrt{2}V$. The violation of $S \leq 2$ shows quantum entanglement between the two photons.

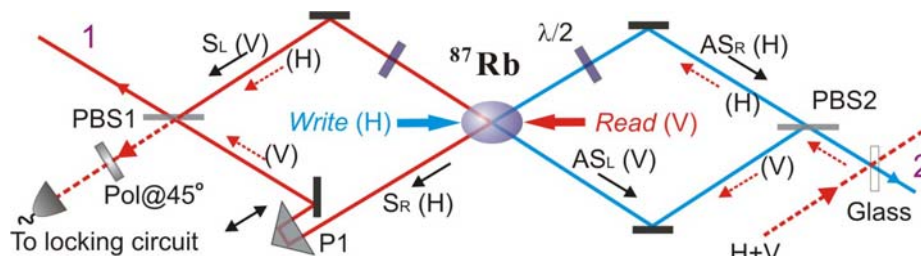
Shown in Supplementary Figure 2, the S parameter is 2.60 ± 0.03 (resulting in a visibility of 92%), at storage time of 500 ns and goes to lower than 2 at 24 μs . The small difference between the measured S and the estimated one should arise from the imperfections of the optics.

2. Phase stabilization method

As discussed in the present paper, the phase in the DLCZ-type functional quantum node¹⁴ should be stabilized in a single-photon Mach-Zehnder interferometer whose arms span the whole communication distance, where a sub-wavelength stability of the transmission channel is needed. When the distance between the communication sites becomes tens of kilometers, the path length fluctuations is extremely large and impossible to stabilize using the passive method. Even for an active stabilization method it is currently experimentally challenging. While in our experiment, since the two-photon Hong-Ou-Mandel-type interferometer is exploited in the entanglement connection, the requirement is to overlap the wave packets of two “messenger” photons at the BSM. Therefore, the stability requirement for our interferometer is on the order of

coherence length of the photons, which is several-meter-long. In our experiment, a Mach-Zehnder interferometer is used at each site to generate the atom-photon entanglement. Here, the only task we need to do is to actively stabilize the phase of the local interferometer. This is a standard technique and can be easily performed with a high precision. We describe this technique as below.

Different from the technique in a previous atom-photon entanglement source²⁰, the current method for phase stabilization is simpler and more stable. Generally, the phase in Eqn. (3) consists of four terms arising from the write beam, the read beam, the anti-Stokes and the Stokes modes. However, since the two spatial modes share the same write and read beams, they always observe a same phase of the write and of the read. So, only the anti-Stokes and Stokes modes contribute to the phase $\phi_1 + \phi_2$, with ϕ_1 (ϕ_2) arising from the path difference between AS_L (S_L) and AS_R (S_R). The present setup provides high-quality entanglement and long-term stability by simply locking the phase of $\phi_1 + \phi_2$. This is an obvious advantage compared with the atom-photon entanglement implemented with two atomic ensembles^{12,20}.



Supplementary Figure 3: Phase stabilization method. The prism P1 is mounted on a piezo and the phase difference between the two arms L and R can be controlled by driving this piezo.

To stabilize the phase $\phi_1 + \phi_2$ in equation (3) actively, a Mach-Zehnder interferometer are used as shown in Supplementary Figure 3. A locking beam with the frequency of read and polarized at 45° is switched on during the 20 ms MOT loading stage and sent into the interferometer at PBS2 by the weak reflection of a glass slice.

This locking beam is overlapped with the two spatial modes L and R . As the anti-Stokes and Stokes light are perpendicularly polarized, the output of the locking beam is from another port of PBS1. After the locking beam goes through a polarizer at 45° , the interference signal can be detected by a photodiode and used to lock the phase $\phi_1 + \phi_2$. During the experimental stage, this locking beam is switched off by an acousto-optical modulator to prevent the collective excitation being destroyed.

Each arm of the Mach-Zehnder interferometer is about 1 meter long in the present setup. With this active locking method, the visibility of the atom-photon entanglement was kept at 92% during the experiment. In contrast, the visibility became nearly random within a few minutes without the locking.

3. The estimation of the precision of local operations

To calculate the precision of local operations in the entanglement swapping, we assume the generated state of the two remote atomic ensembles is a Werner state, since all the mixed state can be transformed to a Werner state by bilateral unitary transformation.

In our experiment, the overall visibilities of the two atom-photon entanglement sources were obtained as $V_I=92\%$ and $V_{II}=90\%$ from measured CHSH parameter via $S = 2\sqrt{2}V$. The relation between the initial visibilities V_I , V_{II} and the final visibility V ($2.26/(2\sqrt{2}) = 80\%$) can be written as $V=p_1^2 p_2(4\eta^2-1)V_I V_{II}/3$ according to Eqn. (5) in Ref. [6], where p_1 and p_2 are the reliabilities of one- and two-qubit operations, and η is the quality of a single-qubit measurement. With the visibilities above, one get $p_1^2 p_2(4\eta^2-1)/3 = 96.6\%$. Assume $\eta=99.5\%$ since the extinction ratio of the polarization analyzer is better than 200:1, $p_1^2 p_2=97.9\%$, so $p_2>97.9\%$, which indicates the precision of local operations. Assume the same precision can be achieved in the further connections and purifications. Actually, this assumption is reasonable since the precision of local operations depends on the quality of optical devices like beam

splitters, polarizers and half-wave plates, whose extinction ratio can be very high.

Plugging $\eta=99.5\%$ into Eqn. (6) in Ref. [6], we obtained a threshold of $p_{2\text{-th}}=95.2\%$ above which future entanglement purification works. When we used the measured precision $p_2=97.9\%$, a fidelity region of $57.7\%=F_{\min}<F<F_{\max}=94.2\%$ was obtained, which means any initial fidelity between this region can be purified up to 94.2% with the help of auxiliary entanglement pairs. With the current precision of local operations, if we do another connection between two entanglement pairs with both fidelities of 94.2%, the connected longer pair has a fidelity of 86.7%, which is in the region of $[F_{\min}, F_{\max}]$. If we have seven nodes with all fidelities of 94.2%, after six connections the finally connected entanglement pair will have a fidelity of 59.8%, still in the region of $[F_{\min}, F_{\max}]$. This estimation shows that the quantum network is scalable with the current precision of local operations, given a sufficiently long lifetime of the generated entanglement pairs.

4. Towards long-distance quantum communication

Following the BDCZ scheme^{6,9}, connecting two of the present building blocks provides a chance to generate entanglement deterministically. Double excitations are “washed” out automatically with this connection by a carefully designed Bell-state measurement.

Considering double emissions, the entangled state generated in the two atomic ensembles is described by

$$|\psi\rangle_{I,II} = \left(\frac{S_{L_I}^\dagger S_{L_{II}}^\dagger + S_{R_I}^\dagger S_{R_{II}}^\dagger}{2} + \frac{S_{L_I}^\dagger S_{R_I}^\dagger + S_{L_{II}}^\dagger S_{R_{II}}^\dagger}{2} \right) |\text{vac}\rangle_{I,II} \quad (\text{S3})$$

where the spatial modes and atomic ensembles are distinguished by subscript (L,R) and (I,II), respectively. The first part is the maximally entangled state needed for further

operation, while the second part is the unwanted two-excitation state coming from second-order excitations.

It is obvious the spurious contributions of two-excitation terms prevent further entanglement manipulation and must be eliminated by some means. However we find that it is not necessary to worry about these terms, because they can be automatically washed out if the BSM in further entanglement swapping is carefully designed.

Let us consider four communication sites I , II , III and IV and assume we have created complex entangled states $|\psi\rangle_{I,II}$ and $|\psi\rangle_{III,IV}$ between sites (I,II) and (I,IV) respectively. Note the atomic ensembles II and III are at the same location. The memory qubits II and III are illuminated simultaneously by read laser pulses. The retrieved anti-Stokes photons are subject to BSM. Note that the arrangement of the PBSs in this BSM is designed to identify Bell state $|\phi^\pm\rangle$ at $|+\rangle/|-\rangle$ polarization basis (in contrast to the BSM used in the paper at $|H\rangle/|V\rangle$ polarization basis), so that the two-photon states converted from the unwanted two-excitation terms are directed into the same output and thus won't induce a coincidence count on the detectors. Conditioned on the coincidence events in this BSM, the memory qubits are projected into a maximally entangled state.

$$|\psi\rangle_{I,IV} = \frac{1}{\sqrt{2}}(S_{L_I}^\dagger S_{L_{IV}}^\dagger + S_{R_I}^\dagger S_{R_{IV}}^\dagger)|\text{vac}\rangle_{I,IV}. \quad (\text{S4})$$

Considering the imperfections in experiments, we find that the coincidence counts prepare the memory qubits into a mixed entangled state of the form $\rho_{I,IV} = p_2\rho_2 + p_1\rho_1 + p_0\rho_0$, where the coefficients p_2 , p_1 and p_0 are determined by the retrieve efficiency and detection efficiency. Here $\rho_2 = |\psi\rangle_{I,IV}\langle\psi|$ is a maximally entangled state, ρ_1 is a maximally mixed state where only one of the four spatial modes has one excitation and ρ_0 is the vacuum state that all the spatial modes are in the ground states. It is easy to see that $\rho_{I,IV}$ is in fact an effectively maximally entangled states,

which can be projected automatically to a maximally entangled state in the entanglement based quantum cryptography schemes. When we implement quantum cryptography via the Ekert protocol²⁹, only the first term ρ_2 can contribute to a coincidence count between the detectors at the two sites and will be registered after classical communication. The maximally mixed state term ρ_1 and the vacuum term ρ_0 have no contribution to the experimental results, and thus $\rho_{I,IV}$ is equivalent to the Bell state $|\psi\rangle_{I,IV}$.

The effectively entangled state can be connected to longer communication distance via further entanglement swapping. A detailed calculation shows that, during the entanglement connection process, the coefficients p_2 , p_1 and p_0 are stable to the first order thanks to the two-photon detection⁶. The time overhead scales quadratically with the communication distance. The entangled state can also be actively purified by use of linear optics quantum purification³⁰.

Supplementary Notes

28. de Riedmatten, H. et al. Direct measurement of decoherence for entanglement between a photon and stored atomic excitation. *Phys. Rev. Lett.* **97**, 113603 (2006).
29. Ekert, Artur K. Quantum cryptography based on Bell's theorem. *Phys. Rev. Lett.* **67**, 661–663 (1991).
30. Pan, J.-W., Gasparoni, S., Ursin, R., Weihs, G. & Zeilinger, A. Experimental entanglement purification of arbitrary unknown states. *Nature* **423**, 417 (2003).